

Infrared study of ion-irradiated N₂-dominated ices relevant to Triton and Pluto: formation of HCN and HNC

M.H. Moore^{a,*} and R.L. Hudson^b

^a Code 691, NASA/Goddard Space Flight Center, Greenbelt, MD 20771, USA

^b Department of Chemistry, Eckerd College, St. Petersburg, FL 33733, USA

Received 28 March 2002; revised 8 August 2002

Abstract

Infrared spectra and radiation chemical behavior of N₂-dominated ices relevant to the surfaces of Triton and Pluto are presented. This is the first systematic IR study of proton-irradiated N₂-rich ices containing CH₄ and CO. Experiments at 12 K show that HCN, HNC, and diazomethane (CH₂N₂) form in the solid phase, along with several radicals. NH₃ is also identified in irradiated N₂ + CH₄ and N₂ + CH₄ + CO. We show that HCN and HNC are made in irradiated binary ice mixtures having initial N₂/CH₄ ratios from 100 to 4, and in three-component mixtures have an initial N₂/(CH₄ + CO) ratio of 50. HCN and HNC are not detected in N₂-dominated ices when CH₄ is replaced with C₂H₆, C₂H₂, or CH₃OH.

The intrinsic band strengths of HCN and HNC are measured and used to calculate $G(\text{HCN})$ and $G(\text{HNC})$ in irradiated N₂ + CH₄ and N₂ + CH₄ + CO ices. In addition, the HNC/HCN ratio is calculated to be ~1 in both icy mixtures. These radiolysis results reveal, for the first time, solid-phase synthesis of both HCN and HNC in N₂-rich ices containing CH₄.

We examine the evolution of spectral features due to acid–base reactions (acids such as HCN, HNC, and HNCO and a base, NH₃) triggered by warming irradiated ices from 12 K to 30–35 K. We identify anions (OCN⁻, CN⁻, and N₃⁻) in ices warmed to 35 K. These ions are expected to form and survive on the surfaces of Triton and Pluto. Our results have astrobiological implications since many of these products (HCN, HNC, HNCO, NH₃, NH₄OCN, and NH₄CN) are involved in the syntheses of biomolecules such as amino acids and polypeptides.

© 2003 Elsevier Science (USA). All rights reserved.

Keywords: Radiation chemistry; Pluto; Triton; Spectroscopy; Ices

1. Introduction

Near-infrared (IR) observations reveal that nitrogen-rich ice containing small amounts of methane (CH₄) and carbon monoxide (CO) is abundant on the surfaces of Pluto and Triton, a moon of Neptune (Cruikshank et al., 1993, Owen et al., 1993). Detailed comparisons between observations and laboratory spectra indicate an N₂ + CH₄ + CO mixture on Triton of 100:0.1:0.05 (Quirico et al., 1999). Frequencies of the observed CH₄ bands confidently indicate that this molecule exists in a diluted state in solid nitrogen at or above 35.6 K, although some regions of pure CH₄ are consistent with bidirectional

reflectance models for the surface. Also observed on Triton, separated from the nitrogen-rich regions, are terrains containing H₂O + CO₂ ices. For Pluto, which has a surface temperature of ~40 K, similar detailed comparisons between observations and laboratory spectra indicate an N₂ + CH₄ + CO mixture of 100:0.5:0.25 (Doute et al., 1999). Here the CH₄ is diluted in N₂, but it is not as segregated as on Triton. IR signatures of either pure CH₄ or CH₄ with a small fraction of nitrogen are also detected, as are regions of nearly pure N₂, and dark regions possibly from processed organics (Grundy and Buie, 2001). Although not excluded from reflectance models fitting Pluto's spectrum, H₂O does not seem to be necessary. For both Pluto and Triton, N₂, CH₄, and CO sublime and condense in a complex manner during their seasonal cycles (Grundy and Stansberry, 2000).

* Corresponding author. Fax: +1-301-286-0440.

E-mail address: ummhm@lepvox.gsfc.nasa.gov (M.H. Moore).

Although both Triton and Pluto are at 35–40 K, their surface ices can still undergo chemical alterations due to the presence of various ionizing radiations. Solar UV photons, the solar wind plasma, and cosmic rays are all present, but it is the cosmic ray source that dominates at the surfaces of Triton and Pluto. The solar UV and wind fluxes are greatly diminished at the distances of Triton and Pluto (30.1 and 39.4 AU, respectively), and any UV photons that do interact with these worlds are absorbed in their tenuous atmospheres (rough UV penetration depth of about 3 $\mu\text{m-atm}$ or less). Ignoring the expected deflection of solar wind plasma (e.g., Bagenal and McNutt, 1989), keV ions will deposit their energy in the upper atmospheres. As a result, some atmospheric chemistry will be induced by the solar UV and wind fluxes, and by Neptune's magnetospheric electron flux as well, in the case of Triton (see discussion by Delitsky and Thompson, 1987, and Krasnopolsky and Cruikshank, 1995). Although products formed from atmospheric photolysis and radiolysis may precipitate onto ice surfaces, influencing the ices' reflectance, the ice chemistry of Triton and Pluto is dominated by the more penetrating radiations, namely the galactic cosmic rays (GCR). Johnson (1989) examined the radiation environment of Pluto and showed that surface doses from cosmic ray bombardment were small per orbit ($\sim 9 \times 10^{-6}$ eV molecule⁻¹ in the top 10 g cm⁻² layer) for MeV protons. The same GCR flux at Triton would result in $\sim 6 \times 10^{-6}$ eV molecule⁻¹ in the top 10 g cm⁻² layer per orbit. Over 4.6 billion years, the accumulated dose for Pluto and Triton is ~ 165 eV molecule⁻¹. For Triton, more complete modeling by Delitsky and Thompson (1987) examined how the GCR dose in the surface depends on the density of the atmosphere. They calculated that over 4.6 billion years, 167–293 eV molecule⁻¹ is deposited in the upper ~ 10 m. For comparison, ices irradiated with only a few eV molecule⁻¹ are expected to form detectable IR signatures of C₂H₆, based on 1-MeV proton radiolysis of H₂O + CH₄ (7:1) (Moore and Hudson, 1998) and 7.3-MeV proton radiolysis of pure CH₄ ice (Kaiser and Roessler, 1998). Typically, organics mixed with ices become “red” after a dose of ~ 100 eV molecule⁻¹ (e.g., Andronico et al., 1987). It is the long-term accumulation of organic radiation products that can alter the average reflectance of icy surfaces and produce detectable IR features of radiation products.

From laboratory studies of energetically processed C- and N-containing ices (e.g., Allamandola, 1988; d'Hendecourt et al., 1986; Foti et al., 1984; Hagen et al., 1979; Johnson, 1989; Khare et al., 1989; Lanzerotti et al., 1987; Moore et al., 1983; Strazzulla et al., 1984; Thompson et al., 1987; and references therein) we know that there is a net loss of hydrogen, and complex and often colored and/or dark organic products are formed. The formation of several CN-bonded species has been documented in IR spectra of a few ion-irradiated N₂-containing icy mixtures (Strazzulla and Palumbo, 2001; Hudson et al., 2001). Irradiated N₂ + H₂O + CH₄ (1:1:1) and N₂ + CH₃OH (1:1) icy mixtures formed new features at 2260, 2168, and 2085 cm⁻¹, which

were attributed to HNCO, and OCN species, and HCN, respectively (Strazzulla and Palumbo, 2001). Similarly a more nitrogen-rich mixture, N₂ + H₂O + CH₄ (100:4:10), showed the same CN features after irradiation (Strazzulla and Palumbo, 2001; Satorre et al., 2001). Hudson et al. (2001) identified the 2168-cm⁻¹ feature as the OCN⁻ ion in both N₂ + H₂O + CH₄ ($\sim 1:1:1$) and N₂ + H₂O + CO (1:5:1); HNCO was shown to form in irradiated N₂ + H₂O + CO. Only one report (Bohn et al., 1994), however, focuses on energetically processed N₂-rich mixtures relevant to the segregated ices of Triton and Pluto. In that paper, IR spectra of UV-photolyzed N₂ + CH₄ (200:1) and N₂ + CH₄ + CO (200:1:1) were measured. The formation of CH₂N₂, CH₃, and C₂H₂ was reported for N₂ + CH₄ ice, along with weaker features characteristic of alkynes and amines. In UV-photolyzed N₂ + CH₄ + CO ice, CH₂N₂, CH₃, C₂H₂, HCO, H₂CO, and (CHO)₂ were identified.

In the present paper, we describe the first systematic IR study of proton-irradiated N₂-rich ices relevant to Triton and Pluto. We chose the mid-IR spectral region since it contains strong diagnostic infrared absorptions of molecules making it the prime region for identification of species, as opposed to the near-IR region, which contains weaker overtone absorption bands. We include results on pure N₂, CH₄, and CO, along with the binary mixtures CO + CH₄, N₂ + CO, and N₂ + CH₄ and the three-component mixture N₂ + CH₄ + CO. These ices were ion-irradiated at 12 K to study the formation and stability of new species. Important goals were to identify new products, to investigate pathways for the synthesis of CN-bonded species, and to consider complications introduced by the presence of CO. To determine likely products participating in pathways, it was necessary to examine 12-K spectra where radicals and other reactive species were isolated prior to their diffusion and reaction as the temperature was raised. In N₂-rich ices containing CH₄ we observed the formation of HCN, HNC, and NH₃. The evolution and stability of these products were followed by warming to $T \geq 35$ K, where OCN⁻, CN⁻, N₃⁻, and NH₄⁺ were identified. We discuss the importance of N₂-rich mixtures containing CH₄ and show that radiation chemistry results in a condensed-phase pathway for the synthesis of several species containing CN bonds. We conclude that similar species are likely to exist on the surfaces of Triton and Pluto and review the current detection of such species in both interstellar and cometary environments. A condensed-phase route to such CN-bonded species (e.g., HCN, HNC, OCN⁻, and CN⁻) has astrobiological significance since similar molecules have been used as precursors for the abiotic synthesis of compounds such as amino acids and the nucleic acid adenine (Oro, 1960).

2. Experimental methods

Details of the experimental setup, ice preparation, IR spectral measurements, cryostat, UV lamp, and proton beam

source have been published (Moore and Hudson, 1998, 2000; Hudson and Moore, 1995). In summary, ice samples were formed by condensation of gas-phase mixtures onto a precooled aluminium mirror at ~ 12 K, although some experiments were performed at slightly higher temperatures. Compositions of the resultant ices were determined from the partial pressures of gases in the original mixtures. The vapor deposition technique produces an intimately mixed ice dominated by α N₂. Most ice films were several micrometers thick, as determined by a laser interference fringe system. IR spectra were recorded as a function of temperature in some experiments, as the ice temperature could be maintained between 12 and 300 K.

Mid-IR spectra (4000 to 400 cm⁻¹) were taken before and after energetic processing of ices by diverting the beam of an FTIR spectrometer (Mattson Instruments) toward the ice-covered mirror, where it passed through the ice before and after reflection at the ice–mirror interface. Typically 60-scan accumulations were used for 4-cm⁻¹ resolution spectra and 120-scan accumulations for 1-cm⁻¹ spectra.

Ices were processed by turning them to face either a beam of 0.8-MeV protons, generated by a Van de Graaff accelerator, or UV photons from a microwave-discharged hydrogen flow lamp. The use of proton irradiation to simulate cosmic-ray bombardment has been discussed in other papers (e.g., Moore et al., 2001; Moore et al., 1983). We used standard relations to estimate a stopping power of 323 MeV cm⁻¹ (Chatterjee, 1987) and a range of ~ 20 μ m ($\sim 0.5 \times 10^{20}$ molecule cm⁻²) for 0.8-MeV protons in solid N₂ (see www.srim.org). Based on this range, we know that incident protons in our experiment passed through the ices and came to rest in the substrate mirror. Dominant radiation-chemical reactions triggered by laboratory 0.8-MeV protons are the same as those triggered by a range of higher MeV GCR protons (up to ~ 110 MeV) that penetrate the top 10 cm ($\sim 10^{23}$ molecule cm⁻²) of the surfaces of Triton and Pluto. Unless otherwise noted, dose calculations are specific to the mass of the dominant molecule in the ice mixture, N₂ (1 eV molecule⁻¹ = 1 eV (28 amu molecule)⁻¹).

Results from several UV-photolysis experiments are included to show similarities to and differences from proton bombardment experiments. Our recent lamp calibrations show that the average incident photon's energy is 7.41 ± 0.23 eV and the flux is 3.1×10^{14} photons cm⁻² s⁻¹. Gerakines et al. (2000) described in detail the methods by which photolytic and radiation doses can be calculated and compared.

Band strengths of HCN and HNC were needed to determine column densities and yields in different radiation experiments. The intrinsic band strength, $A(\text{HCN})$, in cm molecule⁻¹ was determined from the band area $\int \tau(\tilde{\nu}) d\tilde{\nu}$, in cm⁻¹, using

$$A = \frac{\int \tau(\tilde{\nu}) d\tilde{\nu}}{N},$$

where N , the column density (molecule cm⁻²), was calculated from the total film thickness, the gas-phase ratio of N₂/HCN, and the density of N₂ ice (1.027 g cm⁻³, Scott, 1976). We found $A(\nu_3 \text{ HCN}) = 1.1 \times 10^{-17}$ (+0.46, -0.29) cm molecule⁻¹ in N₂ at 12 K.

$A(\text{HNC})$ was estimated indirectly. We observed that during irradiation (or UV photolysis) at 12 K, HCN isomerized to HNC. Assuming each HNC comes from the rearrangement of one HCN, the decrease in band intensity of HCN is directly proportional to the increase in band intensity of HNC. This assumption results in a calculation of a lower limit for $A(\text{HNC})$. A plot of the decreasing area of an HCN band against the increasing area of an HNC band has a slope equal to $A(\text{HNC})/A(\text{HCN})$. Taking $A(\nu_3 \text{ HCN}) = 1.1 \times 10^{-17}$ (+0.46, -0.29) cm molecule⁻¹, we found $A(\nu_3 \text{ HNC}) = 5.1 \times 10^{-18}$ (+5.1, -2.2) cm molecule⁻¹. The average and uncertainty are calculated for $A(\text{HCN})$ from four spectra in one experiment and for $A(\text{HNC})$ from four spectra in two different experiments.

Initial yields of HCN and HNC were calculated by determining the slope of the linear portion of a plot of column density vs energy dose (eV cm⁻²). Initial yields, as opposed to equilibrium abundances, are given since we are interested in product formation from direct interaction of the radiation with the original reactant molecules, and not yields averaged over the course of the entire radiation experiment (see discussion in Gerakines and Moore 2001). The production yield is given as a G -value, the number of molecules formed per 100 eV of energy deposited. We calculated $G(\text{HCN}) = 0.066 \pm 0.014$ and $G(\text{HNC}) = 0.067 \pm 0.007$ in N₂ + CH₄ (100:1) ices; $G(\text{HCN}) = 0.023 \pm 0.002$ and $G(\text{HNC}) = 0.025 \pm 0.001$ in N₂ + CH₄ + CO (100:1:1) ices after a dose of ~ 2 eV molecule⁻¹. The uncertainty is the error in the slope of a linear fit to the data.

Most ice mixtures were irradiated or photolyzed at 12 K, a temperature below the expected surface temperatures of 30–35 K for Triton and Pluto. N₂ and CO sublime rapidly in our 10⁻⁸-torr vacuum when warmed to 35 K since their vapor pressures are in the ranges 10⁻³ and 10⁻⁴ torr, respectively (Honig and Hook 1960). CH₄ is less volatile at 35 K, with a vapor pressure in the range 10⁻⁷ torr. After processing, our ices were warmed and spectra were recorded at 30–35 K. In some cases spectra of less volatile species were recorded up to room temperature.

Reagents used and their purities are as follows: N₂ (Air Products research grade, 99.9995%), ¹⁵N₂ (Aldrich, ¹⁵N₂ 98%), CO (Matheson, 99.99%), CH₄ (Matheson, 99.999%), CD₄ (MSD Isotopes, 99.2% atom D), ¹³CH₄ (Monsanto Research Corp., 99% atom ¹³C), C₂H₂ (Matheson, purified using appropriate ice bath to remove acetone), C₂H₆ (Air Products, CP grade), C₂H₄ (Matheson, 99.99%), CH₃OH (Aldrich, HPLC grade). HCN was synthesized in a vacuum manifold by combining KCN and stearic acid (both from Eastman Kodak) in nearly equal molar ratios and heating to approximately 353 K. The gases released were collected in a glass bulb cooled by liquid N₂. An acetone slush bath at

178 K was used to separate the HCN from impurity gases such as CO₂.

3. Results

3.1. Results at low temperature ($T = 12$ K)

Presentation of our results begins with experiments involving pure N₂, CO, and CH₄ ices. Next, we consider the binary mixtures CO + CH₄, N₂ + CO, and N₂ + CH₄. Finally we examine the more complex three-component mixture, N₂ + CO + CH₄. This provides a self-consistent approach to understanding the chemical results. Experiments comparing IR products in proton-irradiated and UV-photolyzed pure N₂- and CO-ice have been published, as have studies of ion irradiation and UV-photolysis products in pure CH₄. Therefore we combine here our new observations with those previously reported for pure ices to lay the foundation for understanding the mixtures examined.

3.1.1. Pure N₂

Since N₂ has no permanent dipole moment, it has no IR-allowed features. However, the mid-IR spectrum of solid N₂ at 12 K shows a weak forbidden transition at 2328.2 cm⁻¹ that is significantly enhanced by the presence of CO₂ (Sandford et al., 2001, and Bernstein and Sandford, 1999). It is also known that bombardment of pure solid N₂ with either 4 keV Ne/Ne⁺ (Tian et al., 1988) or 120 eV N atoms (Khabashesku et al., 1997) produces the N₃ radical (1657 cm⁻¹), an electrically neutral species with an unpaired electron in its outer orbital. N₃, like many free radicals, can be stabilized in low-temperature matrices, but reacts quickly during warming. In our experiments, the N₃ radical was observed after proton bombardment of solid N₂, but not after UV photolysis. Thus N₃ is a signature of radiolysis. In a recent paper (Hudson and Moore, 2002) N₃ radical formation in both pure N₂ and N₂-rich ices is examined. The N₂-rich ices studied in our current experiments are listed in Table 1 along with the positions of the observed N₃ band.

Green luminescence was observed from N atoms during radiolysis of pure N₂, and on warming irradiated N₂. This luminescence has been characterized through many experiments (e.g., Peyron and Broida, 1959). No luminescence was detected during UV photolysis experiments or on warming UV-photolyzed N₂ ices.

3.1.2. Pure CO

Major products identified in proton-irradiated CO ice were CO₂ at 2343 cm⁻¹ and C₃O₂ at 2242 cm⁻¹. In UV-photolyzed CO, the major product was CO₂ (spectra not shown). Table 1 lists major radiation products and their peak positions. In a recent paper by Gerakines and Moore (2001), a detailed comparison of mid-IR spectra of pure CO before and after radiolysis and photolysis was presented. Included were details of the formation and thermal stability

of C₃O₂, a molecule that can polymerize to form a more stable dark reddish-brown material. Formation yields for C₃O₂ were $G(\text{C}_3\text{O}_2)_{\text{radiolysis}} = 0.2$ and $G(\text{C}_3\text{O}_2)_{\text{photolysis}} = 0.01$.

3.1.3. Pure CH₄

Figure 1 shows the mid-IR spectrum of pure solid CH₄ at 12 K before and after processing with both protons and UV photons. Bands of CH₄, at 3011 cm⁻¹ (ν_3) and 1298 cm⁻¹ (ν_4), dominate the spectrum of the freshly deposited ice. After processing, dominant new IR features are due to C₂H₆, C₂H₄, and C₃H₈. Also detected was a weak band at 3269 cm⁻¹, attributed to C₂H₂. Each numbered feature in Fig. 1 is identified in Table 1. Identifications were made by matching the position and relative intensity of each product band with appropriate solid-phase reference spectra.

We compared our results with earlier work on processed CH₄ ice. Kaiser and Roessler (1998) studied solid methane after irradiation with 9-MeV α -particles and 7.3-MeV protons. They analyzed irradiated CH₄ using mid-IR spectroscopy and probed gases released during warm-up through mass spectrometry. New molecules were identified in the IR (e.g., C₂H₆, C₂H₄, and C₂H₂), along with some less abundant, larger mass species. Gerakines et al. (1996) used IR to examine the complex photochemistry of pure CH₄ at 10 K and identified C₂H₆, C₂H₄, and C₃H₈ as major products. Baratta et al. (2002) compared the loss of CH₄ after UV photolysis and 30-keV He⁺ bombardment. They showed that at <20 eV (16 amu)⁻¹ both processes give similar results, but at higher doses, impinging ions modify the entire sample while UV photons cause fewer modifications since they are absorbed at increasingly smaller depths. Other studies, e.g. Davis and Libby (1964) and Calcagno et al. (1985), formed and analyzed room-temperature residues from processed CH₄ ice. These last two studies are less relevant to our low-temperature radiation chemistry focus, but are important for documenting the overall loss of H and the evolution of pure CH₄ toward a dark, carbon-rich film.

3.1.4. CO + CH₄

Experiments were performed on CO + CH₄ ice mixtures and are included here for the sake of completeness (spectra not shown). A CO + CH₄ (100:1) mixture was ion-irradiated, and a 50:1 CO + CH₄ ice was photolyzed. Interesting new observations were of bands at 1380 and 1127 cm⁻¹, probably from ketene (Moore et al., 1965), at 619 cm⁻¹ for CH₃ (Milligan and Jacox, 1967a), at 2026 cm⁻¹ for HCCO (Forney et al., 1995), and at 2489, 1859, and 1090 cm⁻¹ for the formyl radical, HCO (Milligan and Jacox, 1964). Table 1 lists major products and their peak positions.

3.1.5. N₂ + CO

New features appearing in processed solid N₂ + CO (100:1) at 12 K are shown in Fig. 2. The spectrum before processing contains only the bands of CO at 2139 cm⁻¹ and ¹³CO at 2092 cm⁻¹. Comparing results from proton-irradi-

Table 1
New species identified in ice experiments at 12 K

Ice	Peak #	Position		Spectrum	Ice	Peak #	Position		Spectrum
		cm ⁻¹ (μm)	Assignment				cm ⁻¹ (μm)	Assignment	
N ₂ ^a		1657 (6.035)	N ₃ radical	p+	N ₂ + CO	1	2348 (4.259)	CO ₂	p+ and UV
CO ^b		2398 (4.170)	C ₃ O ₂	p+ and UV	(100:1)	2	2253 (4.438)	C ₃ O ₂	p+
		2340 (4.274)	¹² CO ₂	p+ and UV		3	2235 (4.474)	N ₂ O	p+ and UV
		2280 (4.386)	¹³ CO ₂	p+ and UV		4	1934 (5.171)	OCN radical	p+
		2242 (4.460)	C ₃ O ₂	p+ and UV		5	1874 (5.336)	NO	p+
		1990 (5.025)	C ₂ O	p+ and UV		6	1657 (6.035)	N ₃ radical	p+
CH ₄	1	3269 (3.059)	C ₂ H ₂	p+ and UV	7	1615 (6.192)	NO ₂	p+ and UV	
	2	2976 (3.360)	C ₂ H ₆	p+ and UV	8	1291 (7.746)	N ₂ O	p+ and UV	
	3	2960 (3.378)	C ₃ H ₈	p+ and UV	9	1040 (9.615)	O ₃	p+ and UV	
	4	2941 (3.400)	C ₂ H ₆	p+ and UV	N ₂ + CH ₄ (100:1)	1	3565 (2.805)	HNC	p+ and UV
	5	2883 (3.469)	C ₂ H ₆	p+ and UV		2	3286 (3.043)	HCN	p+ and UV
	6	1463 (6.835)	C ₂ H ₆	p+ and UV		3	3270 (3.058)	C ₂ H ₂	UV
	7	1436 (6.964)	C ₂ H ₄	p+ and UV		4	2980 (3.356)	C ₂ H ₆	p+ and UV
	8	1373 (7.283)	C ₂ H ₆ , C ₃ H ₈	p+ and UV		5	2096 (4.771)	HCN, CH ₂ N ₂	p+ and UV
	9	951 (10.515)	C ₂ H ₄	p+		6	1798 (5.562)	HCN ₂ radical	p+ and UV ^c
	10	821 (12.180)	C ₂ H ₆ , C ₂ H ₄ , C ₃ H ₈	p+ and UV		7	1657 (6.061)	N ₃ radical	p+
	11	748 (13.369)	C ₃ H ₈	p+		8	1407 (7.107)	CH ₂ N ₂	p+ and UV
	12	608 (16.447)	CH ₃ radical	p+ and UV ^d		9	971 (10.30)	NH ₃	p+
	13	534 (18.727)	C ₂ H ₅ radical	p+		10	881 (11.35)	CH ₂ N ₂	p+ and UV
CO + CH ₄ p+ (100:1) UV (50:1)		3262 (3.066)	C ₂ H ₂	p+ and UV		11	747 (13.39)	HCN	p+
		2489 (4.018)	HCO radical	p+ and UV		12	611 (16.37)	CH ₃ radical	p+
		2343 (4.268)	CO ₂	p+ and UV		13	561 (17.82)	C ₂ H ₅ radical	p+
		2241 (4.462)	C ₃ O ₂	p+ and UV	N ₂ + CO + CH ₄ ^e (100:1:1)		3565 (2.805)	HNC	p+
		2026 (4.936)	HCCO radical	p+ and UV			3285 (3.044)	HCN	p+
		1989 (5.028)	C ₂ O	p+			2976 (3.360)	C ₂ H ₆	p+ and UV
		1859 (5.379)	HCO radical	p+ and UV			2348 (4.259)	CO ₂	p+ and UV
		1736 (5.760)	H ₂ CO	p+ and UV			2266 (4.413)	HNCO	p+
		1727 (5.790)	HCOCH ₃	p+ and UV			2235 (4.474)	N ₂ O	p+ and UV
		1526 (6.553)	C ₃ O ₂	p+			2096 (4.771)	HCN, CH ₂ N ₂	p+ and UV
		1498 (6.676)	H ₂ CO	p+ and UV			1798 (5.562)	HCN ₂ radical	p+ and UV
		1429 (6.998)	HCOCH ₃	p+			1933 (5.173)	OCN radical	p+
		1380 (7.246)	H ₂ CCO	p+ and UV			1861 (5.373)	HCO radical	p+ and UV
		1349 (7.413)	HCOCH ₃	p+ and UV			1657 (6.035)	N ₃ radical	p+
		1127 (8.873)	H ₂ CCO	p+ and UV			1407 (7.107)	CH ₂ N ₂	p+ and UV
		1122 (8.913)	HCOCH ₃	p+ and UV			1089 (9.183)	HCO	p+ and UV
		1090 (9.174)	HCO radical	p+ and UV			971 (10.30)	NH ₃	p+
		659 (15.151)	CO ₂	p+ and UV			880 (11.36)	CH ₂ N ₂	p+ and UV
		619 (16.155)	CH ₃ radical	p+ and UV			743 (13.46)	HCN	p+
		551 (18.149)	C ₃ O ₂	p+			662 (15.11)	CO ₂	p+ and UV
		541 (18.584)	C ₃ O ₂	p+			611 (16.37)	CH ₃ radical	p+ and UV

^a Hudson and Moore (2001).

^b Gerakines and Moore (2001).

^c UV formed CH₃ from Gerakines et al. (1996).

^d UV photolysis species from Elsila et al. (1997).

^e UV photolysis species from Bohn et al. (1994).

ated and UV-photolyzed ices shows that both processes form CO₂ efficiently. Products N₂O, NO₂, and NO are numbered in Fig. 2 and identified in Table 1. N₃ and OCN radicals were formed only in ion-irradiated N₂ + CO. Major features identified in our UV-photolyzed ice (spectra not shown) are consistent with those reported by Elsila et al. (1997). Although C₃O₂ was efficiently formed in pure, irradiated CO ices, in N₂-rich ices only a weak feature at 2253 cm⁻¹ is identified with matrix-isolated C₃O₂. This feature at 2253 cm⁻¹ and other weak features in the region 2200 cm⁻¹ agree in position with a more intense complex

band formed in irradiated N₂ + CO (1:1), attributed to C₃O₂.

3.1.6. N₂ + CH₄

Mid-IR spectra of N₂ + CH₄ (100:1) before and after processing are shown in Figs. 3 and 4. In the unprocessed ice, the bands of CH₄ at 3014 cm⁻¹ (ν₃) and 1302 cm⁻¹ (ν₄) dominate. Small features were detected due to the forbidden transition of N₂ (2328 cm⁻¹) and to H₂O (3726 and 1598 cm⁻¹) and CO₂ (2349 cm⁻¹) impurities. New features (e.g., HNC, HCN, NH₃, and the N₃ radical, along with diazometh-

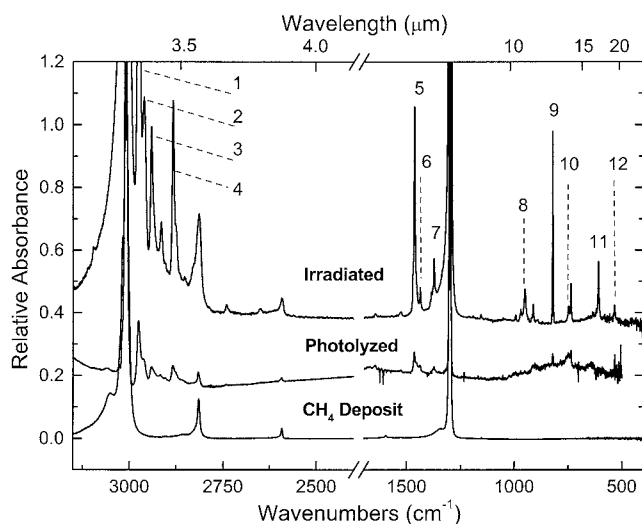


Fig. 1. Mid-IR spectrum of pure CH₄ (thickness $\sim 4 \mu\text{m}$) deposited at 12 K, compared with the same ice after proton irradiation to a dose of $\sim 1 \text{ eV}$ ($16 \text{ amu molecule}^{-1}$). The spectrum of photolyzed CH₄ at 12 K from Gerakines et al. (1996) is included for comparison. Positions and identifications of numbered features are listed in Table 1. New molecules identified after processing are C₂H₂, C₂H₆, C₂H₄, and C₃H₈.

ane, CH₂N₂) are numbered in Figs. 3 and 4 and identified in Table 1. Although C₂H₂, C₂H₄, C₂H₆, and C₃H₈ are formed in irradiated pure CH₄-ice, only a small signature of C₂H₆ is detected in the IR spectrum of processed N₂ + CH₄ (100:1) mixtures, where most CH₄ molecules are surrounded by N₂.

The spectrum of ion-irradiated N₂ + CH₄ shows features identified as HNC, HCN, NH₃, and the N₃ radical, along with CH₂N₂ (Moore et al., 1965) and the CH₃ (Milligan and Jacox, 1967a), CH₂CH₃ (Pacansky et al., 1981) and HCN₂ (Ogilvie, 1968) radicals. These results demonstrate a con-

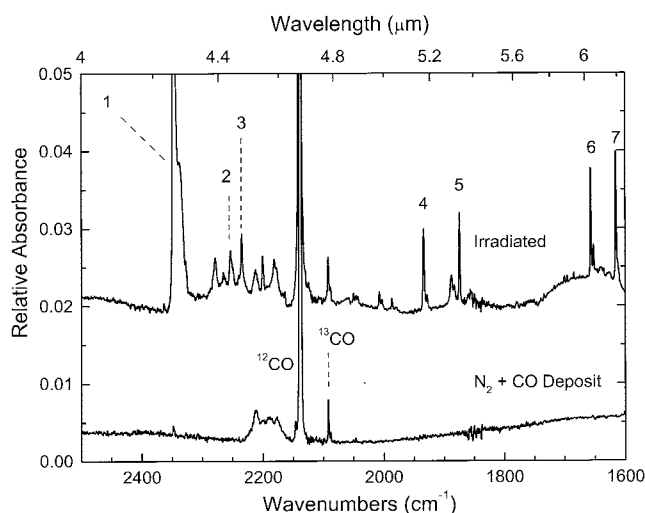


Fig. 2. Mid-IR spectrum from 2500 to 1600 cm⁻¹ of N₂ + CO (100:1) (thickness $\sim 3.5 \mu\text{m}$) deposited at 12 K, compared with that same ice after proton irradiation to a dose of $\sim 1 \text{ eV molecule}^{-1}$. Identifications and band positions of numbered features are given in Table 1.

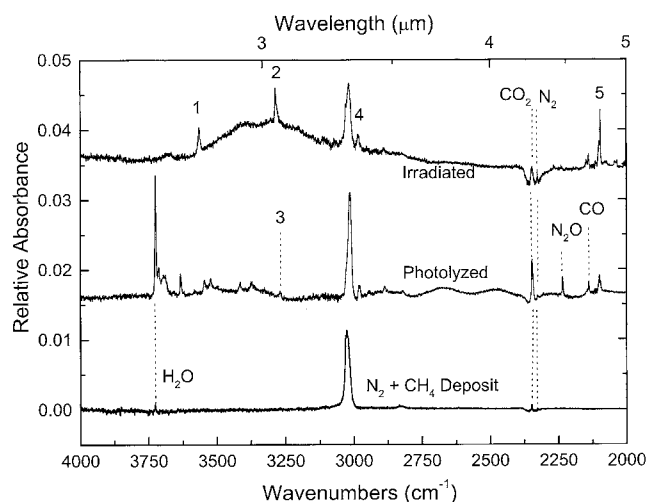


Fig. 3. Spectra from 4000 to 2000 cm⁻¹ of N₂ + CH₄ (100:1) (thickness $\sim 3 \mu\text{m}$) before and after processing at 12 K. This spectral region contains the ν_3 CH₄ band. New features formed in the ice after irradiation (dose of $\sim 1 \text{ eV molecule}^{-1}$) are numbered and identified in Table 1. For comparison, a spectrum of N₂ + CH₄ (100:1) simultaneously deposited and photolyzed over a 2-h period is also shown. Absorption features due to HNC and HCN at 3565 and 3286 cm⁻¹, along with CH₂N₂ and HCN at 2096 cm⁻¹, are detected in the irradiated mixture.

densed-phase pathway for the formation of acids HNC and HCN and a base (NH₃) in N₂-rich ices containing CH₄.

The spectrum in Figs. 3 and 4 for the UV-processed N₂ + CH₄ was recorded after simultaneous photolysis and deposition for $\sim 2 \text{ h}$. The resulting ice thickness was $\sim 6 \mu\text{m}$. The major products we detected, CH₂N₂, C₂H₂, and the CH₃ radical, were the same as those reported by Bohn et al.

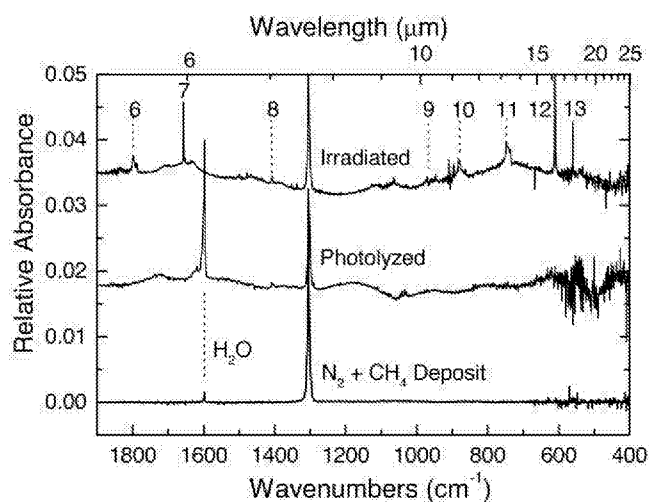


Fig. 4. Spectra from 1900 to 400 cm⁻¹ of N₂ + CH₄ (100:1) (thickness $\sim 3 \mu\text{m}$) before and after processing at 12 K. This spectral region contains the ν_4 CH₄ band. New features formed in the ice after irradiation (dose of $\sim 1 \text{ eV molecule}^{-1}$) are numbered and identified in Table 1. For comparison, a spectrum of photolyzed N₂ + CH₄ (100:1) is also shown. New molecules in the irradiated ice include HCN (747 cm⁻¹), CH₂N₂ (1407 and 881 cm⁻¹), and NH₃ (971 cm⁻¹).

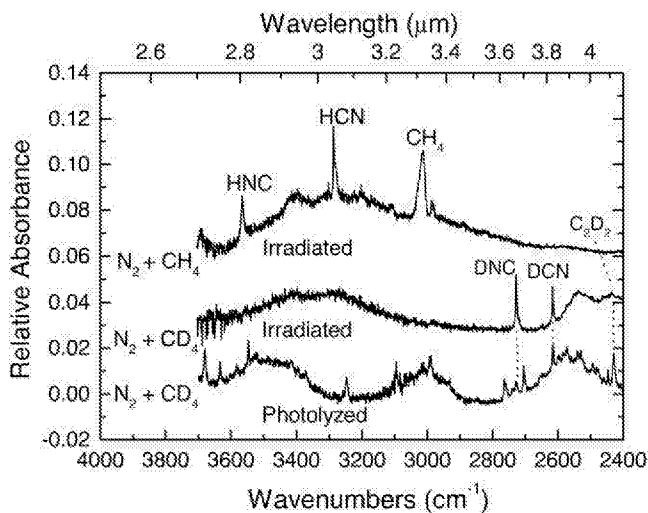


Fig. 5. The mid-IR spectrum of irradiated $N_2 + CH_4$ (100:1) at 12 K shows formation of HNC and HCN at 3565 and 3286 cm^{-1} , respectively. Both irradiated and UV-photolyzed $N_2 + CD_4$ (100:1) shows formation of DNC and DCN at 2726 and 2615 cm^{-1} , respectively. (MeV proton dose was ~ 1 eV molecule $^{-1}$, UV exposure was $\sim 7 \times 10^{17}$ UV photons cm^{-2}) The ν_3 CD_4 band lies at 2258 cm^{-1} , outside the region of this plot. A feature due to C_2D_2 is also identified.

(1994) for an $N_2 + CH_4$ ice (200:1). After photolysis we also identified C_2H_6 in the 100:1 mixture at 12 K. Weak features in the Bohn et al. (1994) experiment also point to the possible presence of HNC and HCN, but it is difficult to interpret the presence or absence of such weak signatures without additional work. Our photolyzed $N_2 + CH_4$ sample was also examined for the formation of HCN and HNC, but potential signatures were very weak.

Identification of the ν_3 bands of HCN and HNC in N_2 matrices was made by comparison to an $N_2 + HCN$ (2000:1) ice, which had been proton-irradiated to form HNC (reference spectrum shown in Fig. 6). Our HNC and HCN band positions were consistent with those reported in matrix isolation studies by King and Nixon (1968) and Milligan and Jacox (1967a, 1967b).

The relative intensities of different HCN bands have been studied in the past and are relevant to our work. For example, Masterson and Khanna (1990) reported n and k values for pure solid HCN at 60 K and showed that its strongest band was at 3130 cm^{-1} (ν_3). The ν_3 feature of HCN is also the most intense band when it is diluted in N_2 . For an N_2/HCN ratio of 100, we measured the relative intensities at 3286 cm^{-1} (ν_3), 2096 cm^{-1} (ν_1), and 747 cm^{-1} (ν_2) as 1:0.3:0.8.

One problem encountered was the secure identification of the strongest band of HCN since its position was near the ν_3 band of C_2H_2 . As already mentioned, the 3286 cm^{-1} (ν_3) feature of HCN was easily detected in irradiated $N_2 + CH_4$ ice spectra. In photolyzed $N_2 + CH_4$ a weak band at 3270 cm^{-1} was observed and attributed to acetylene (C_2H_2) (Bohn et al., 1994). Solid solutions of C_2H_2 in an N_2 matrix showed the ν_3 monomeric C_2H_2 band at 3282 cm^{-1} and the

ν_5 fundamental at 748 and 743 cm^{-1} (Bagdanskis et al., 1970). However, nearly identical positions are found for the 3286 cm^{-1} (ν_3) and 746 cm^{-1} (ν_2) bands of HCN. Therefore, it was necessary to explore in more detail the HCN identification using various isotopomers.

A comparison of irradiated $N_2 + CH_4$ and $N_2 + CD_4$ (100:1) is shown in Fig. 5, along with the spectrum of photolyzed $N_2 + CD_4$. Features identified with HNC and HCN are at 3565 and 3286 cm^{-1} (respectively) in the $N_2 + CH_4$ ice. Both irradiated and photolyzed $N_2 + CD_4$ had features at 2728 and 2616 cm^{-1} assigned to DNC and DCN, respectively (Milligan and Jacox, 1967a; King and Nixon, 1968). These assignments are facilitated by the well-separated IR positions of DCN, DNC, and C_2D_2 . Good evidence that acetylene is not a major contributor in an irradiated $N_2 + CH_4$ (100:1) mixture is the presence of only a very weak ν_3 C_2D_2 feature at 2435 cm^{-1} (Bagdanskis and Bulanin, 1972) in Fig. 5. This point is important because it implies that HCN is the major source of the 3286 cm^{-1} feature in irradiated $N_2 + CH_4$. Further support of the HNC and HCN identifications comes from our examination of an irradiated mixture of $^{15}N_2 + CH_4$ (100:1) (spectrum not shown) and the identification of $H^{15}NC$ at 3553 cm^{-1} and $HC^{15}N$ at 3285 cm^{-1} (i.e., ^{15}N -shifts of -12 and -1). Similarly, irradiated $N_2 + ^{13}CH_4$ (100:1) showed the formation of $HN^{13}C$ and $H^{13}CN$ at 3562 and 3268 cm^{-1} , respectively (i.e., ^{13}C -shifts of -3 and -18 cm^{-1}). All shifts observed in the hydrogen isocyanide and hydrogen cyanide isotopomers are consistent with those found in an argon matrix (Miekle and Andrews, 1990) (^{15}N -shifts of -12 and -1 cm^{-1} and ^{13}C -shifts of -1 and -17 cm^{-1}).

Fig. 6 shows that HCN and HNC were detected in irra-

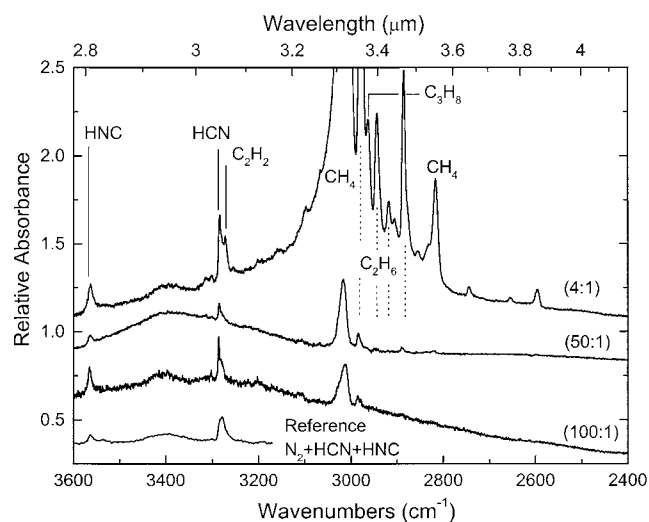


Fig. 6. Mid-IR ice spectra of irradiated $N_2 + CH_4$ with N_2/CH_4 ratios of 100, 50, and 4. HNC and HCN were detected after irradiation at 12 K for all concentrations of CH_4 . Each ice received ~ 1 eV molecule $^{-1}$. The ice with the higher concentration of CH_4 also formed the most C_2H_2 , C_2H_6 , and C_3H_8 . Our reference spectrum of HNC and HCN isolated in N_2 is also shown.

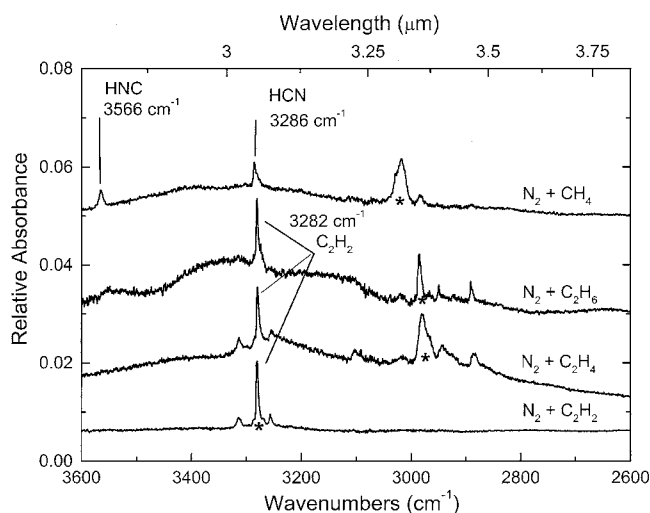


Fig. 7. Spectra of N_2 -rich ices containing CH_4 , C_2H_6 , C_2H_4 , or C_2H_2 are compared after irradiation. All had an N_2 /organic ratio of 100 and were $\sim 3 \mu m$ thick. Each received a dose of $\sim 1 eV \text{ molecule}^{-1}$. Only the CH_4 -containing ice formed HNC and HCN after irradiation. C_2H_6 - and C_2H_4 -containing ices formed C_2H_2 . Little change was detected in the $N_2 + C_2H_2$ ice. The * shows the position of the reactant organic in each spectrum.

diated $N_2 + CH_4$ for three different N_2/CH_4 ratios: 100, 50, and 4. Also detected at all ratios were two features of CH_2N_2 , at 2096 and 1406 cm^{-1} . The strengths of the aliphatic hydrocarbon features due to C_2H_6 and C_3H_8 increased as the initial concentration of CH_4 increased. The C_2H_2 absorption at 3273 cm^{-1} was best seen in the experiment with an N_2/CH_4 ratio of 4, although its presence in more dilute mixtures is seen as a shoulder of the HCN absorption at 3286 cm^{-1} .

In irradiated N_2 -rich ices, HCN and HNC did not form when CH_4 was replaced by other simple aliphatic hydrocarbons. A comparison of products in irradiated 100:1 mixtures of N_2 with CH_4 , C_2H_6 , C_2H_4 , or C_2H_2 is presented in Fig. 7. Irradiated $^{14}N_2 + C_2H_6$ ($\nu_1 C_2H_6$ at 2986 cm^{-1}) and $^{15}N_2 + C_2H_6$ (spectrum not shown) both formed a band at 3282 cm^{-1} attributed to C_2H_2 . Other products detected between 2600 and 400 cm^{-1} were C_2H_4 and CH_4 . Irradiated $N_2 + C_2H_4$ ($\nu_9 C_2H_4$ at 3104 cm^{-1}) formed C_2H_2 , along with C_2H_6 , C_2H_4 , and CH_4 . Irradiated $N_2 + C_2H_2$ ($\nu_3 C_2H_2$ at 3282 cm^{-1}) formed several new weak bands.

To determine trends in product formation, we examined $N_2 + CD_4$ (100:1) ices as a function of radiation dose. These experiments were done with CD_4 , as opposed to CH_4 , to remove the problem of confusing adjacent IR features (e.g., overlapping HCN and C_2H_2 bands in the region $3290\text{--}3270 \text{ cm}^{-1}$), so that band areas could be determined without curve fitting. Fig. 8 plots trends in product formation and loss of CD_4 over an extended dose period.

The band areas of DCN, DNC, and CD_2N_2 showed growth and saturation with increasing radiation dose. The ν_4 band of CD_4 (at 993 cm^{-1}) decreased with increasing dose as CD_4 was destroyed. Based on our 12-K experiment, about half of the CD_4 was destroyed after a dose of $\sim 3 eV$

molecule^{-1} . A similar dose on Triton and Pluto would accumulate after ~ 80 million years of exposure (Johnson, 1989). However, due to the complex transport of volatiles on these icy objects, there may be no stable CH_4 so that application of these results is not straightforward.

Finally, in addition to the acids HNC and HCN, the base NH_3 was detected at 971 cm^{-1} (ν_2). This is the strongest band of NH_3 isolated in an N_2 matrix. Its band position and intensity in our work are consistent with matrix isolation studies (Lundell et al., 1998 and references therein) and our own reference spectrum of $N_2 + NH_3$ (100:1) (not shown).

3.1.7. $N_2 + CH_4 + CO$

HNC and HCN also were detected at 3565 and 3285 cm^{-1} , respectively, in irradiated $N_2 + CH_4 + CO$ (100:1:1), demonstrating formation of these products in the presence of CO. Fig. 9 shows the mid-IR spectrum in the range $3600\text{--}2600 \text{ cm}^{-1}$ for $N_2 + CH_4 + CO$, for $N_2 + CH_4$, and for two other ices (discussed in Section 3.1.8.). After irradiation of $N_2 + CH_4 + CO$, the N_3 radical was detected at 1656 cm^{-1} , and CH_2N_2 bands were seen at 2096 and 1407 cm^{-1} . Table 1 lists observed features from 4000 to 400 cm^{-1} , which includes radiation products from both $N_2 + CO$ and $N_2 + CH_4$ ices along with NH_3 and isocyanic acid, HNC. This acid formed only when both CH_4 and CO were present in an N_2 -rich ice. Spectral features of HNC and CH_2N_2 in the region $2275\text{--}1975 \text{ cm}^{-1}$ are shown in Fig. 10.

Other products from photolyzed $N_2 + CH_4 + CO$ (100:1:1) (spectrum not shown) included CH_2N_2 , C_2H_6 , HCO, and CO_2 . These are the same products reported by Bohn et al. (1994) for a UV-photolyzed 200:1:1 mixture. Band positions and identifications of UV-products given in Table 1 come from both our results and those of Bohn et al. (1994).

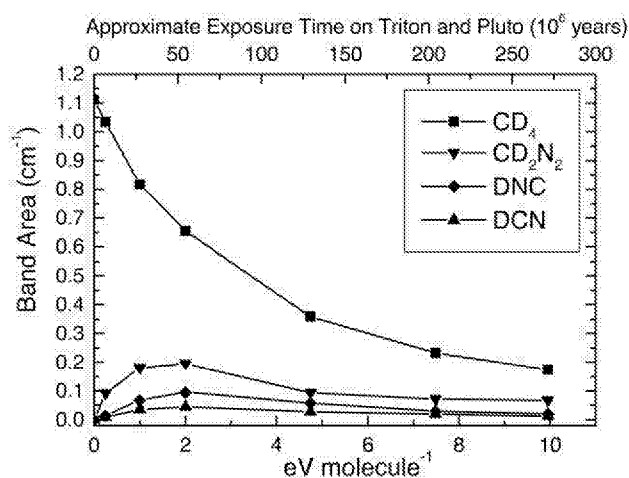


Fig. 8. Change in the ν_3 band areas of DNC and DCN and the ν_2 band area of CD_2N_2 as a function of energy dose in 12-K $N_2 + CD_4$ (100:1) ice (thickness $\sim 8 \mu m$). Decrease in ν_4 band area of CD_4 is also shown. A fourth-order polynomial curve is drawn through the CD_4 data. The initial area of the CD_4 band is reduced 50% after $\sim 3 eV \text{ molecule}^{-1}$, which is equivalent to ~ 80 million years exposure on the surface of Pluto or Triton.

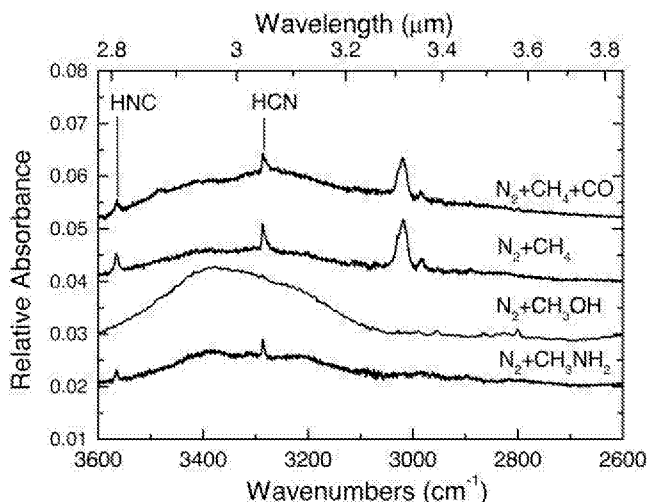


Fig. 9. Infrared signatures of HNC and HCN were detected in N_2 -rich ices containing $CH_4 + CO$, CH_4 , or methylamine (CH_3NH_2) at 12 K after irradiation to ~ 1 eV molecule $^{-1}$. Each ice had an N_2/C -containing molecule ratio of 100:1 and a thickness of ~ 3 μm . HNC and HCN were not detected in $N_2 + CH_3OH$ after irradiation.

Ion-irradiated $N_2 + CH_4 + CO$ ices for three $N_2/(CH_4 + CO)$ ratios (50, 5, and 0.5) showed HNC and HCN only when the initial ratio was 50. When the ratio was 5 or 0.5, the dominant products included aliphatic hydrocarbons, CO_2 , C_3O_2 , and a molecule with a $C=O$ bonded feature at 1720 cm^{-1} , probably acetaldehyde.

3.1.8. Other routes to HCN and HNC

Although irradiated N_2 ices containing CH_4 led to HNC, HCN, and CH_2N_2 , other routes to these species were investigated. As mentioned before, irradiated $N_2 + C_2H_6$ did not produce HNC, HCN, or CH_2N_2 . Instead, the observed major reaction was the synthesis of C_2H_4 and C_2H_2 as hydrogen was lost, with a change from $C-C$ to $C=C$ to $C\equiv C$ bonding: $H_3C-CH_3 \rightarrow H_2C=CH_2 \rightarrow HC\equiv CH$.

Since in the search for formation pathways we were not limited by the requirement that the ice composition be relevant to Triton or Pluto, we examined the possible synthesis of HNC and HCN in dilute N_2 matrices containing methanol (CH_3OH) and methylamine (CH_3NH_2). First we examined CH_3OH , a relatively abundant molecule in comets and interstellar ices. CH_3OH has one CH_3 group connected to OH through a $C-O$ bond. Previously the 2096 cm^{-1} band of HCN was reported in the IR spectrum of irradiated $N_2 + CH_3OH$ (1:1) (Strazzulla et al., 2001). However, in the dilute mixtures studied in this paper, irradiated $N_2 + CH_3OH$ (100:1) ice did not show IR features of HNC, HCN, or CH_2N_2 . Instead, bands for H_2CO at 1738 and 1499 cm^{-1} and CO at 2140 cm^{-1} showed that the major reaction was the loss of hydrogen and the accompanying change from $C-O$ to $C=O$ to $C\equiv O$ bonding: $H_3C-OH \rightarrow H_2C=O \rightarrow C\equiv O$. Fig. 9 compares the mid-IR spectrum (in the spectral range from 3600 to 2600 cm^{-1}) of proton-

irradiated $N_2 + CH_3OH$ (100:1) at 12 K with that of irradiated $N_2 + CH_4$ and $N_2 + CH_4 + CO$.

The other molecule examined was CH_3NH_2 , which has a CH_3 group bonded to an NH_2 group through a $C-N$ bond. After irradiation of $N_2 + CH_3NH_2$ (100:1), HNC and HCN were identified (see Fig. 9). The reaction path probably led from $C-N$ to $C=N$ to $C\equiv N$ bonding: $H_3C-NH_2 \rightarrow H_2C=NH \rightarrow HC\equiv N$ (and $HN\equiv C$). Weak signatures of the intermediate product, CH_2NH , detected near 1066 , 1129 , 1354 , 1452 , and 1639 cm^{-1} (spectrum in this range is not shown) are consistent with this proposed reaction path.

3.2 Results at $T \geq 30$ K

The ion-irradiation studies of $N_2 + CH_4$ (100:1) and $N_2 + CH_4 + CO$ (100:1:1) described above were performed at ~ 12 K, below the 35 – 40 K thought to be relevant for Triton and Pluto (Quirico et al., 1999; Doute et al., 1999). Table 1 lists all of the new products trapped in the N_2 matrix at 12 K. The list includes four CN-bonded species, six radicals, NH_3 , and hydrocarbons. This group contains both acids and bases. Knowing the identity of these reactive species provides important clues for understanding possible chemical reaction pathways during diffusion, as the matrix becomes less rigid with warming. In our experiments, the intensities of sharp IR features of molecules such as HNC, HCN, and HNCO were diminished greatly at 30 K, which is evidence for chemical reactions triggered by warming.

Fig. 10 compares spectra in the ranges 3600 – 3200 and 2300 – 1950 cm^{-1} for irradiated $N_2 + CH_4 + CO$ (100:1:1)

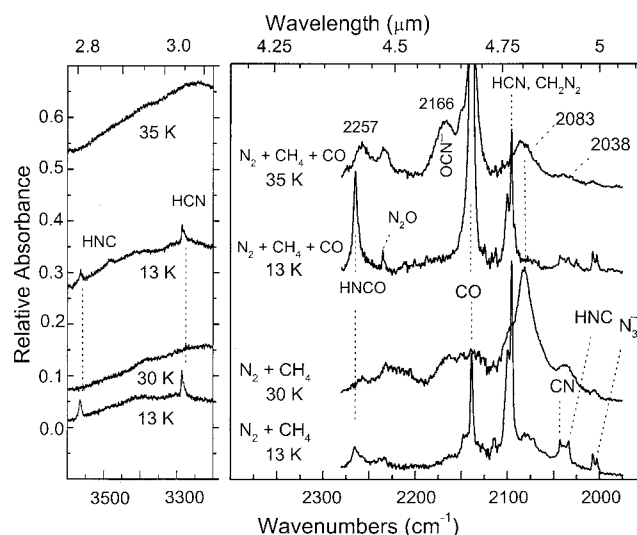


Fig. 10. IR spectra of $N_2 + CH_4$ (100:1) and $N_2 + CH_4 + CO$ (100:1:1) ices at 12 K after irradiation to ~ 1.5 and 1 eV molecule $^{-1}$, respectively, compared to a spectrum of the same ice warmed to 35 K. Increasing the temperature triggered acid–base reactions resulting in changes in spectral features. Relatively sharp molecular features of the acids HNC, HCN, and HNCO, along with the CN radical and the free N_3^- ion, disappeared with warming. Absorption bands at 2166 , 2083 , and 2038 cm^{-1} appeared at 35 K and are identified with the OCN^- , CN^- , and N_3^- ions, respectively.

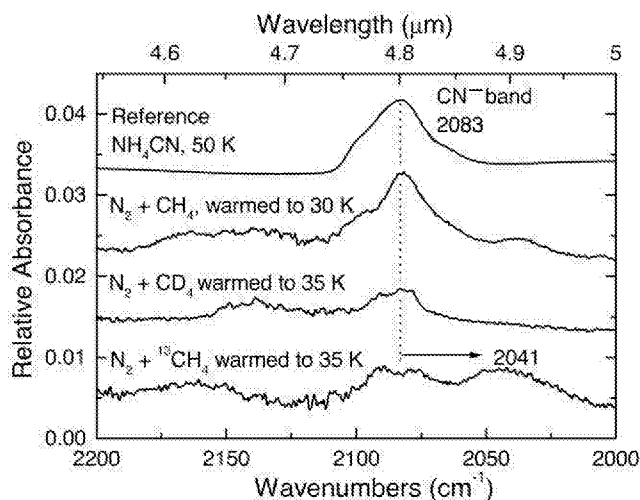


Fig. 11. The feature at 2083 cm^{-1} formed in $\text{N}_2 + \text{CH}_4$, (100:1), after the irradiated ice was warmed to 35 K. This band is compared with a reference spectrum of NH_4CN at 50 K (P.A. Gerakines, personal communication, 2002). In addition, we compare the band at 2083 cm^{-1} in $\text{N}_2 + \text{CH}_4$ with features from two experiments with isotopically labeled molecules. Processed $\text{N}_2 + \text{CD}_4$ showed CN^- in the same position, but $\text{N}_2 + {}^{13}\text{CH}_4$ developed a band, ${}^{13}\text{CN}^-$, shifted to 2041 cm^{-1} . Each irradiated ice received a dose of $\sim 1\text{ eV molecule}^{-1}$.

and $\text{N}_2 + \text{CH}_4$ (100:1) ices at 12 K and the same ices warmed to 30–35 K. Sharp features at 12 K attributed to HNC (3565 and 2030 cm^{-1}) and HCN (3285 cm^{-1}) and the 2096 cm^{-1} feature attributed to both HCN and CH_2N_2 were not seen after warming. In addition, features at 2266 cm^{-1} (HNCO), 2040 cm^{-1} (the CN radical), and 2003 cm^{-1} (the free azide ion, N_3^- (Tian et al., 1988)) disappear after warming.

The relatively sharp feature of HNCO was detected in the $\text{N}_2 + \text{CH}_4 + \text{CO}$ irradiated ice at 12 K. A small feature attributed to HNCO in the $\text{N}_2 + \text{CH}_4$ ice comes from CO formation from a CO_2 impurity in the original ice mixture. At 35 K, HNCO is replaced by a broad weaker feature at $\sim 2257\text{ cm}^{-1}$ and the 2166 cm^{-1} band of the OCN^- ion. The formation of OCN^- is consistent with a reaction involving HNCO and NH_3 , and is direct evidence of an acid–base reaction triggered by raising the temperature.

The 2083 cm^{-1} band formed in irradiated $\text{N}_2 + \text{CH}_4$ (100:1) and $\text{N}_2 + \text{CH}_4 + \text{CO}$ (100:1:1) ices warmed from 12 to 35 K is evidence of a second acid–base reaction. In this case, HCN and most likely NH_3 react to form ammonium cyanide, NH_4^+ and CN^- . Fig. 11 compares the 2083 cm^{-1} band of irradiated $\text{N}_2 + \text{CH}_4$ (100:1) at 30 K with a spectrum of NH_4CN produced by warming an HCN + NH_3 ice from 13 K to 50 K (P.A. Gerakines, private communication). The CN-stretch feature of NH_4CN is a good match to our 2083 cm^{-1} band. Spectral studies of pure NH_4CN at 77 K list a $\text{C}\equiv\text{N}$ stretch at 2095 cm^{-1} (Kanesaka et al., 1984). Furthermore, our identification of the 2083 cm^{-1} band with the CN^- ion is supported by isotopic substitution experiments. Fig. 11 shows that irradiated $\text{N}_2 + \text{CD}_4$

(100:1) ice, warmed to 35 K, formed a band at 2084 cm^{-1} with essentially no shift in position from the CH_4 -containing ice. This implies that the vibration corresponding to the 2083 cm^{-1} band has no contamination from hydrogen. Fig. 11 also shows that similarly irradiated and warmed ice containing ${}^{13}\text{CH}_4$ forms a band near 2041 cm^{-1} , a shift of -42 cm^{-1} from the ${}^{12}\text{C}$ position. A ${}^{15}\text{N}_2 + \text{CH}_4$ irradiated and warmed ice (spectrum not shown) formed a new band near 2047 cm^{-1} , a shift of -36 cm^{-1} from the ${}^{14}\text{N}$ position. These shifts are consistent with those found for CN^- ions in neon matrices by Forney et al. (1992) (${}^{13}\text{CN}^-$ shift of -42 cm^{-1} and C^{15}N^- shift of -31 cm^{-1}). In summary, the 2083 cm^{-1} band is attributed to the CN^- ion (most likely NH_4^+ is the cation).

The weak broad feature at 2038 cm^{-1} in irradiated $\text{N}_2 + \text{CH}_4$ (100:1) and $\text{N}_2 + \text{CH}_4 + \text{CO}$ (100:1:1) ices, warmed to 30–35 K (Fig. 10), is evidence for an azide ion, N_3^- . The azide band is weaker than the OCN^- or CN^- bands, and therefore its identification is not as secure. The free (isolated) azide anion can be identified at 2003 cm^{-1} in both 12-K irradiated ice mixtures (Fig. 10), based on IR studies of bombarded N_2 ice by Tian et al. (1988). (An anion is an atom or group of atoms that carries a negative charge.) They observed that during annealing, the peak at 2003 cm^{-1} decreased as the matrix warmed and sublimed. We observed the same trend during warming along with the formation of a broad weak band at 2038 cm^{-1} , a position consistent with the 2037 cm^{-1} frequency of azides in a KBr lattice (Theophanides and Turrell, 1967). The difference of 39 cm^{-1} between CN^- and N_3^- peak positions increases to 73 cm^{-1} for the ${}^{15}\text{N}$ -labeled ions and is consistent with the increase for these species calculated from matrix experiments. (See Forney et al. (1992) for CN^- values and Tian et al. (1988) for N_3^- values.) These identifications are consistent with formation of the azide anion in an irradiated $\text{N}_2 + \text{NH}_3$ ice where the cation, NH_4^+ , is easy to identify (Hudson et al., 2001). Our observation that a band grows in intensity near 1460 cm^{-1} during the warming of irradiated $\text{N}_2 + \text{CH}_4$ ice is also consistent with NH_4^+ , but since the region 1460 cm^{-1} overlaps with the ν_8 band of C_2H_6 the NH_4^+ identification is less firm. To summarize, the feature 2038 cm^{-1} is assigned to the N_3^- ion.

Results obtained after warming irradiated ices of $\text{N}_2 + \text{CH}_4 + \text{CO}$ (100:1:1) show that OCN^- , CN^- , and N_3^- are part of the residual material above the sublimation temperatures of N_2 , CH_4 , and CO . The infrared positions and FWHM of these anions is given in Table 2. Fig. 12 shows spectra (in the region $2150\text{--}1925\text{ cm}^{-1}$) of irradiated $\text{N}_2 + \text{CH}_4 + \text{CO}$ (100:1:1) warmed from 30 to 200 K after irradiation at 12 K. The ion OCN^- is at 2163 cm^{-1} , CN^- at 2083 cm^{-1} , and N_3^- at 2038 cm^{-1} . We show the warm-up of this ice to demonstrate the higher temperature stability of these ions. All three were detected at 150 K; OCN^- is still detected at 200 K. The relative intensities of these ions are affected by initial concentrations of CH_4 and CO in the ice, the thickness of the ice, and the warming rate. The role that

Table 2
Band positions and width for identified anions

Anion	Irradiated ice			
	N ₂ + CH ₄ + CO		N ₂ + CH ₄	
	Peak position (cm ⁻¹)	FWHM (cm ⁻¹)	Peak position (cm ⁻¹)	FWHM (cm ⁻¹)
Cyanate, OCN ⁻	2166	25		
Cyanide, CN ⁻	2083	21	2081	20
Azide, N ₃ ⁻	2038	20	2036	14

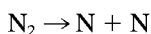
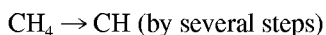
the substrate plays in the stability of these ions at higher temperature is unknown.

4. Discussion

4.1. Mechanisms

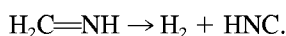
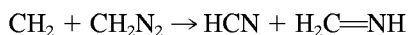
We have shown that HCN and HNC form in irradiated N₂ + CH₄ where the N₂/CH₄ ratio varied from 100 to 4, and in irradiated N₂ + CH₄ + CO (100:1:1) ices. N₂ ices containing other aliphatics such as C₂H₆, a longer saturated hydrocarbon, or C₂H₄ and C₂H₂, doubly- and triply-bonded molecules respectively, did not show HCN and HNC after irradiation.

Several explanations can be conceived for the production of HCN and HNC in our N₂ + CH₄ experiments. It might be possible that CH radicals, formed on radiolysis of CH₄, could react with N atoms, made from N₂, as follows:



Some of the HCN produced could then isomerize to give the observed HNC. The main problem with this mechanism is that only small concentrations of CH and N radicals are expected in our experiments. This means that it is unlikely that CH and N would ever encounter one another in an ice, so that the radical–radical reaction leading to HCN will be unimportant.

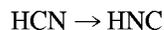
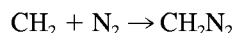
A second possible mechanism for HCN formation is suggested by the work of Moore and Pimental (1965) who observed HCN after photolysis of N₂ + CH₂N₂ mixtures. Their reaction pathway involved formation of CH₂ from CH₄, and their subsequent “attack” on CH₂N₂ in the following sequence:



These reactions explained the presence of both HCN and HNC in photolyzed N₂ + CH₂N₂ mixtures. To search for

these reactions in our experiments, we first checked that ion-irradiated methylamine (CH₃NH₂) would form CH₂NH and that CH₂NH would then be a source for both HNC and HCN. Fig. 9 shows the detection of HNC and HCN in the spectrum of irradiated N₂ + CH₃NH₂ (100:1). This experiment supports the role played by CH₂NH. However, in our irradiated N₂ + CH₄ (100:1) ices CH₂N₂ is itself a reaction product, not a starting material. As such it is unlikely that CH₂ and CH₂N₂, both at low concentrations, would encounter each other. As before, we expect little, if any, HCN from these reactions, with any contribution certainly diminishing as the N₂/CH₄ ratio increases.

As an alternative to these two mechanisms for HCN formation, we offer the work of Maier et al. (1996). In a comprehensive study, they probed the potential energy surface of CH₂N₂ isomers using both experimental and theoretical methods. Diazomethane was shown to rearrange to nitrilimine (HCNNH), and from there to a loose HN ··· HCN complex. As this complex can decompose to NH radicals and HCN, we are led to an intramolecular pathway from CH₂N₂ to HCN. The sequence is as follows:



Because this sequence is intramolecular, once CH₂N₂ is reached the subsequent reactions will occur regardless of the initial N₂/CH₄ ratio. Thus we fully expect HCN and HNC formation on Solar System objects, such as Pluto and Triton, where the N₂:CH₄ ratio may be far higher than in our experiments.

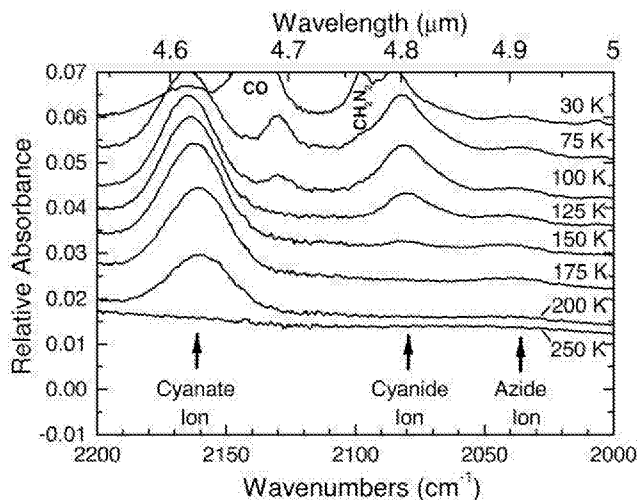
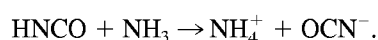
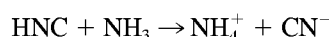
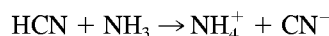


Fig. 12. Infrared spectra in the region 2100 cm⁻¹ show the stability of bands of OCN⁻, CN⁻, and N₃⁻ as a function of temperature. These ions form at 30–35 K in N₂ + CH₄ + CO (100:1:1) ice irradiated to ~1 eV molecule⁻¹. The OCN⁻ band is still seen at 200 K.

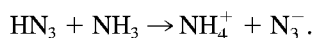
In passing we note that this last set of reactions does not apply to the other hydrocarbons we studied. For example, spectra of proton-irradiated $N_2 + C_2H_6$ ices failed to show IR features of CH_3CHN_2 , diazoethane, whose spectrum is known (Seburg and McMahon, 1992). As the diazo compound did not form, the above reactions imply that no rearrangement to HCN is expected, and indeed no HCN (or HNC) was seen. The observed reaction sequence for C_2H_6 in $N_2 + C_2H_6$ ices appeared to be hydrogen loss as $C_2H_6 \rightarrow C_2H_4 \rightarrow C_2H_2$.

4.2. Temperature effects

IR spectra of 12-K irradiated ices warmed to ~ 30 K showed that relatively sharp features of acids (HCN, HNC, and HNCO) decreased, and bands of OCN^- and CN^- grew, along with a broad feature consistent with NH_4^+ near 1460 cm^{-1} . These changes support the following acid–base reactions:



A broad band for N_3^- was also observed to form when irradiated ices were warmed. One source is the pairing of free N_3^- ions as the matrix material is diminished and diffusion occurs. In addition, a likely reaction occurs in the presence of hydrazoic acid (HN_3) to form N_3^- :



Currently we have only a tentative identification of HN_3 in our irradiated ices, since its strongest band in N_2 matrices lies under the CO band.¹ In summary, we observe extensive acid–base chemistry triggered by warming.

Finally, we note that in contrast to these results for warmed $N_2 + CH_4$ ices, our $N_2 + CO$ mixtures (N_2/CO ratios of 100 or 1) did not form cyanate, cyanide, azide, or ammonium ions when warmed to 35 K. This was not surprising since neither an acid nor a base, like NH_3 , was observed in irradiated $N_2 + CO$ mixtures. Rather than ions, it was carbon suboxide, C_3O_2 , that remained during warming of $N_2 + CO$ samples to $T > 100$ K.

5. Relevance to icy surfaces

A highlight of our study of low-temperature, N_2 -dominated chemistry is the radiation synthesis of nearly equal concentrations of HCN and HNC when CH_4 is present or when both CH_4 and CO are present. This is the first dem-

onstration of condensed-phase pathways to these molecules in realistic Triton/Pluto surface ices. The icy origin of these acids, along with HNCO and possibly HN_3 , sets the stage for reactions with NH_3 to form NH_4^+ , OCN^- , CN^- , and N_3^- as diffusion occurs during warming. Since these ions are thermally more stable than the volatile reactants (N_2 , CH_4 , and CO), they may accumulate on the surfaces of Triton and Pluto and be good candidates for future mid-IR observations. Similar laboratory radiolysis studies are currently underway to identify products in CH_4 - and CO-rich ices with varying concentrations of N_2 (work in progress in our laboratory), and in N_2 -rich ices containing both CH_4 and H_2O (Satorre et al., 2001; Strazzulla and Palumbo, 2001), since terrains on Pluto and Triton may also include these ices.

The radiation chemistry we observed in N_2 -rich laboratory ice mixtures may also be relevant to the chemistry expected in some interstellar ices. N_2 forms most efficiently in interstellar regions where H_2 rather than atomic H exists. Theoretical models of interstellar ice grain chemistry (Tielens and Hagen, 1982; d'Hendecourt et al., 1985) also predict that molecules such as CO, O_2 , and some CO_2 will form and condense along with N_2 . This apolar ice may form as a separate layer on grains (Ehrenfreund et al., 1998). Another likely nonpolar species is CH_4 . Currently, only indirect evidence exists for condensed N_2 mixed with CO, O_2 , and CO_2 (Elsila et al., 1997). Plausible interstellar ratios of N_2/CO , N_2/O_2 , etc. associated with a range of possible environments include N_2 -rich ices.

Observational evidence exists for the presence, in both interstellar regions and comets, of some of the molecular products we report in this paper. Considering first the acids, HCN is one of the more abundant nitrogen-bearing species detected in dense interstellar clouds. In addition, cold interstellar molecular clouds have large HNC/HCN ratios (0.2–1, Ohishi and Kaifu, 1998). In comets, a typical HCN abundance relative to water is $2\text{--}10 \times 10^{-3}$, and HCN is considered a parent species. The HNC/HCN ratio ranges from 0.06 to 0.2 (Irvine, 1996, 1999; Biver et al., 1997; Hirota et al., 1999) depending on the comet and its distance from the Sun. The origin of HNC may be a combination of a native and an extended source (see, e.g., Rodgers and Charnley, 1998). HNCO and NH_3 are detected in both interstellar hot core regions and in cometary comae; NH_3 is also found in dense clouds surrounding protostars (see, e.g., review by Ehrenfreund and Charnley, 2001). These species, identified from gas-phase observations, are expected to condense as icy mantles on cold grain surfaces. Our experimental results demonstrate that in addition to any gas-phase source, a condensed-phase pathway to the formation of these species exists in N_2 -rich ices containing CH_4 and CO. In particular, HNC and HCN form in nearly equal concentrations.

Observations of cold icy grains of embedded protostars show several condensed-phase products we report in this paper. Solid NH_3 is one definite candidate (Gibb et al.,

¹ Confirmation of HN_3 synthesis using appropriate isotopically labeled starting materials is in progress.

2001, Dartois and d'Hendecourt, 2001, and references therein). But detecting NH_3 ice is difficult since its major features overlap with those of H_2O and the silicate band. Of 16 sources, Gibb et al. (2001) showed that 4 have a change in slope at $8.5 \mu\text{m}$ and peak at $9 \mu\text{m}$ that could be attributed to ammonia (the remaining sources have only upper limits). In addition, the prominent feature at 2165 cm^{-1} in IR spectra is assigned to the OCN^- ion (see, e.g., Hudson et al., 2001, and references therein). It is also possible that a contributor to the unidentified absorption band of 1460 cm^{-1} observed toward embedded protostars is the ion NH_4^+ (see, e.g., Demyk et al., 1998). Although the actual N_2 or NH_3 budget in molecular clouds is not well determined; the existence of OCN^- ion supports the idea that low-temperature pathways, similar to those we describe in this paper, occur on cold icy grains.

Radiation processing of N_2 -rich ices on Triton and Pluto could provide an endogenous source of HNC, HCN, HNCO, NH_3 , NH_4^+ , OCN^- , CN^- , and N_3^- . The presence of these molecules would suggest the possibility of interesting prebiotic chemistry. It is well known that many of these species are involved in reactions producing biomolecules. The role of HCN and its derivatives in prebiotic evolution has been discussed by many authors (see, e.g., Matthews, 1995; Oro and Lazcano-Araujo, 1981). Wöhler (1828) and Dunitz et al. (1998) studied the instability of NH_4OCN and its conversion to urea. Draganic et al. (1985) studied the radiation chemistry of solutions of HCN and NH_4CN and the formation of amino acids. More recently, the instability of NH_4CN , in the presence of H_2O and NH_3 was examined by Levy et al. (2000). They found that adenine, guanine, and a set of amino acids dominated by glycine are formed after storage for 25 years at temperatures as low as -78 C . Because it is not clear to what extent any of these prebiotic syntheses would progress at temperatures relevant to Triton and Pluto, this area requires more work.

Evidence for CN-bonded species exists for a variety of other Solar System objects. Along with observed HNC and HCN in cometary coma, there is the detection of a $2.2\text{-}\mu\text{m}$ feature on outer Solar System surfaces, which is suggested to be evidence for the overtone mode of $\text{C}\equiv\text{N}$. For example, this feature is seen on some D-class asteroids, in the dust of some comets, on Iapetus, and in the rings of Uranus (Cruikshank et al., 1991). If a condensed-phase route to HCN, HNC, and other CN-bonded species plays a significant role in Solar System objects, then our work implies a formation region rich in N_2 ices containing CH_4 , but devoid of H_2O .

An opportunity to look closely at Triton and Pluto for evidence of HCN, HNC, and the more stable ion signatures of OCN^- , CN^- , N_3^- , and NH_4^+ will require the resolution and wavelength coverage proposed for NGST, a future IR mission. Detecting and mapping these species may help determine if Pluto and Triton will be targets of future astrobiology missions. The New Horizons Mission is scheduled to make the first reconnaissance of Pluto as early as

2015. However, its proposed spectroscopy is shortward of $2.5 \mu\text{m}$. Therefore, future laboratory work on the near-IR band positions and band strengths of cyanates, cyanide, azides, and polymers of hydrogen cyanide is needed. Understanding the radiation chemistry of remote worlds with N_2 -rich icy surfaces may provide support for the icy origin of HCN and HNC from similarly processed N_2 -rich segregated cometary ices. This scenario would strengthen the idea that comets contain interesting biomolecules.

Acknowledgments

Both authors acknowledge NASA funding through NRA 344-33-01 and 344-02-57. RLH acknowledges support from NASA grant NAG-5-1843. We thank Perry Gerakines for the NH_4CN spectrum resulting from his experiments. Claude Smith and Steve Brown are thanked for their expertise in ensuring adequate beam intensity on the Van de Graaff at Goddard. We thank Professor Robert J. McMahon (University of Wisconsin) for data on methyldiazomethane, and we thank Scott Sandford and Max Bernstein (NASA/Ames) for spectral details of photolyzed $\text{N}_2 + \text{CH}_4$ discussed in Bohn et al. (1994).

References

- Allamandola, L.J., Sandford, S.A., Valero, G.J., 1988. Photochemical and thermal evolution of interstellar/precometary ice analogs. *Icarus* 76, 225–252.
- Andronico, G., Baratta, G.A., Spinella, F., Strazzulla, G., 1987. Optical evolution of laboratory-produced organics: applications to Phoebe, Iapetus, outer belt asteroids and cometary nuclei. *Astron. Astrophys.* 184, 333–336.
- Bagdanskis, N.I., Bulanin, M.O., Fedeev, Yu. V., 1970. Infrared spectra of acetylene in low-temperature matrices, I. *Opt. Spectrosc.* 29, 367–371.
- Bagdanskis, N.I., Bulanin, M.O., 1972. Infrared spectra of acetylene in matrices at low temperatures, II. *Opt. Spectrosc.* 32, 275–277.
- Bagenal, F., McNutt, R., 1989. The solar wind interaction with Pluto's atmosphere. *J. Geophys. Res. Lett.* 16, 1229–1232.
- Baratta, G.A., Leto, G., Palumbo, M.E., 2002. A comparison of ion irradiation and UV photolysis of CH_4 and CH_3OH . *Astron. Astrophys.* 384, 343–349.
- Bernstein, M.P., Sandford, S.A., 1999. Variations in the strength of the infrared forbidden 2328.2 cm^{-1} fundamental of solid N_2 in binary mixtures. *Spectrochim. Acta* 5, 2455–2466.
- Biver, N. and 11 co-authors 1997. Evolution of the outgassing of Comet Hale-Bopp (C/1995 01) from radio observations. *Science* 275, 1915–1918.
- Bohn, R.B., Sandford, S.A., Allamandola, L.J., Cruikshank, D.P., 1994. Infrared spectroscopy of Triton and Pluto ice analogs: the case for saturated hydrocarbons. *Icarus* 111, 151–173.
- Calciogno, L., Foti, G., Torrisi, L., 1985. Fluffy layers obtained by ion bombardment of frozen methane: experiments and applications to saturnian and uranian satellites. *Icarus* 63, 31–38.
- Chatterjee, A., 1987. in: Farhatziz and Rodgers, M.A.J. (Eds.), *Radiation Chemistry*. New York.
- Cruikshank, D.P., Allamandola, L.J., Hartmann, W.K., Tholen, D.J., Brown, R.H., Matthews, C.N., Bell, J.F., 1991. Solid $\text{C}\equiv\text{N}$ bearing material on outer Solar System bodies. *Icarus* 94, 345–353.

- Cruikshank, D.P., Roush, T.L., Owen, T.C., Geballe, T.R., de Bergh, C., Schmitt, B., Geballe, T.R., Bartholomew, M.J., 1993. Ices on the surface of Triton. *Science* 261, 742–745.
- Dartois, E., d'Hendecourt, L., 2001. Search for NH₃ ice in cold dust envelopes around YSOs. *Astron. Astrophys.* 365, 144–156.
- Davis, D.R., Libby, W.F., 1964. Positive ion chemistry: high yields of heavy hydrocarbons from solid methane by ionizing radiation. *Science* 144, 991–992.
- Delitsky, M.L., Thompson, W.R., 1987. Chemical processes in Triton's atmosphere and surface. *Icarus* 70, 354–365.
- Demyk, K., Dartois, E., d'Hendecourt, L., Jourdain de Muizon, M., Heras, A.M., Breittflner, M., 1998. Laboratory identification of the 4.62 μm solid state absorption band in the ISO-SWS spectrum of RAFGL 7009S. *Astron. Astrophys.* 339, 553–560.
- d'Hendecourt, L.G., Allamandola, L.J., Greenberg, J.M., 1985. Time dependent chemistry in dense molecular clouds. *Astron. Astrophys.* 152, 130–150.
- d'Hendecourt, L.G., Allamandola, L.J., Grim, R.J.A., Greenberg, J.M., 1986. Time dependent chemistry in dense molecular clouds. II. Ultraviolet photoprocessing and infrared spectroscopy of grain mantles. *Astron. Astrophys.* 158, 119–134.
- Doute, S., Schmitt, B., Quirico, E., Owen, T.C., Cruikshank, D.P., de Bergh, C., Geballe, T.R., Roush, T.L., 1999. Evidence for methane segregation at the surface of Pluto. *Icarus* 142, 421–444.
- Draganic, Z.D., Draganic, I.G., Azamar, J.A., Vujosevic, S.I., Berber, M.D., Negronmendoza, A., 1985. Radiation-chemistry of over-irradiated aqueous-solutions of hydrogen-cyanide and ammonium cyanide. *J. Mol. Evol.* 21, 356–363.
- Dunitz, J.D., Harris, K.D.M., Johnston, R.L., Kariuki, B.M., MacLean, E.J., Psallidas, K., Schweizer, W.B., Tykwinski, R.R., 1998. New light on an old story: the solid-state transformation of ammonium cyanate into urea. *J. Am. Chem. Soc.* 120, 13274–13275.
- Ehrenfreund, P., Boogert, A., Gerkines, P., Tielens, A., 1998. Apolar ices. *Faraday Discuss.* 109, 463–474.
- Ehrenfreund, P., Charnley, S.B., 2001. Organic molecules in the interstellar medium, comets and meteorites: a voyage from dark clouds to the early Earth. *Annu. Rev. Astron. Astrophys.* 38, 427–483.
- Elsila, J., Allamandola, L.J., Sandford, S.A., 1997. The 2140 cm⁻¹ (4.673 microns) solid CO band: the case for interstellar O₂ and N₂ and the photochemistry of nonpolar interstellar ice analogs. *Astrophys. J.* 479, 818–838.
- Forney, D., Thompson, W.E., Jacox, M.E., 1992. The vibrational spectra of molecular ions isolated in solid neon. IX. HCN⁺, HNC⁺, and CN⁻. *J. Chem. Phys.* 97, 1664–1674.
- Forney, D.W., Jacox, M.E., Thompson, W.E., 1995. The infrared and near-infrared spectra of HCC and DCC trapped in solid neon. *J. Mol. Spectrosc.* 170, 178–214.
- Foti, G., Calcagno, L., Sheng, K.L., Strazzulla, G., 1984. Micrometre-sized polymer layers synthesized by MeV ions impinging on frozen methane. *Nature* 310, 126–128.
- Gerakines, P.A., Schutte, W.A., Ehrenfreund, P., 1996. Ultraviolet processing of interstellar ice analogs. *Astron. Astrophys.* 312, 289–305.
- Gerakines, P.A., Moore, M.H., Hudson, R.L., 2000. Carbonic acid production in H₂O + CO₂ ices: UV photolysis vs. proton bombardment. *Astron. Astrophys.* 357, 793–800.
- Gerakines, P.A., Moore, M.H., 2001. Carbon suboxide in astrophysical ice analogs. *Icarus* 154, 372–380.
- Gibb, E.L., Whittet, D.C.G., Chiar, J.E., 2001. Searching for ammonia in grain mantles toward massive young stellar objects. *Astrophys. J.* 558, 702–716.
- Grundy, W.M., Buie, M.W., 2001. Distribution and evolution of CH₄, N₂, and CO ices on Pluto's surface: 1995 to 1998. *Icarus* 153, 248–263.
- Grundy, W.M., Stansberry, J.A., 2000. Solar gardening and the seasonal evolution of nitrogen ice on Triton and Pluto. *Icarus* 148, 340–346.
- Hagen, W., Allamandola, L., Greenberg, J., 1979. Interstellar molecule formation in grain mantles: the laboratory analog experiments, results and implications. *Astrophys. Space Sci.* 65, 215–240.
- Hirota, T., Yamamoto, S., Kawaguchi, K., Sakamoto, A., Ukita, N., 1999. Observations of DNC and HN¹³C in dark cloud cores. *Astrophys. J.* 520, 895–900.
- Honig, R.E., Hook, H.O., 1960. Vapor pressure data for common gases. *RCA Rev.* 21, 360–368.
- Hudson, R.L., Moore, M.H., 1995. Far-IR spectral changes accompanying proton irradiation of solids of astrochemical interest. *Radiat. Phys. Chem.* 45, 779–789.
- Hudson, R.L., Moore, M.H., Gerakines, P.A., 2001. The formation of the cyanate ion (OCN⁻) in interstellar ice analogs. *Astrophys. J.* 550, 1140–1150.
- Hudson, R.L., Moore, M.H., 2002. The N₃ radical as a discriminator between ion-irradiated and UV-photolyzed astronomical ices. *Astrophys. J.* 568, 1095–1099.
- Irvine, W.M., 1996. Spectroscopic evidence for interstellar ices in Comet Hyakutake. *Nature* 383, 418–420.
- Irvine, W.M., 1999. The composition of interstellar molecular clouds. *Space Sci. Rev.* 90, 203–218.
- Johnson, R.E., 1989. Effect of irradiation on the surface of Pluto. *J. Geophys. Res. Lett.* 16, 1233–1236.
- Kaiser, R.I., Roessler, K., 1998. Theoretical and laboratory studies on the interaction of cosmic-ray particles with interstellar ices. III. Suprathermal chemistry-induced formation of hydrocarbon molecules in solid methane (CH₄), ethylene (C₂H₄), and acetylene (C₂H₂). *Astrophys. J.* 503, 959–975.
- Kanesaka, I., Kawahara, H., Kiyokawa, Y., Tsukamoto, M., Kawai, K., 1984. The vibrational spectrum of the ammonia–hydrogen cyanide system and the normal coordinate analysis of NX₄CN (X = H or D). *J. Raman Spectrosc.* 15, 327–330.
- Khabashesku, V.N., Margrave, J.L., Waters, K., Schultz, J.A., 1997. Matrix isolation Fourier transform infrared spectroscopic study of energetic nitrogen fluxes applied to fabrication of nitride thin films. Observation of N₃ radical and quantitative estimation of matrix-isolated N atoms. *J. Appl. Phys.* 82, 1921–1924.
- Khare, B.N., Thompson, W.R., Murray, B.G.J.P.T., Chyba, C., Sagan, C., 1989. Solid organic residues produced by irradiation of hydrocarbon-containing H₂O and H₂O/NH₃ ices—irradiation spectroscopy and astronomical implications. *Icarus* 79, 350–361.
- King, C., Nixon, E.R., 1968. Matrix-isolation study of the hydrogen cyanide dimer. *J. Chem. Phys.* 48, 1685–1695.
- Krasnopolsky, V.A., Cruikshank, D.P., 1995. Photochemistry of Triton's atmosphere and ionosphere. *J. Geophys. Res.* 100, 21271–21286.
- Lanzerotti, L.J., Brown, W.L., Marcantonio, K.J., 1987. Experimental study of erosion of methane ice by energetic ions and some considerations for astrophysics. *Astrophys. J.* 313, 910–919.
- Levy, M., Miller, S.L., Brinton, K., Bada, J.L., 2000. Prebiotic synthesis of adenine and amino acids under Europa-like conditions. *Icarus* 145, 609–613.
- Lundell, J., Krajewska, M., Räsänen, M., 1998. Matrix isolation fourier transform infrared and *ab initio* studies of the 193-nm-induced photodecomposition of formamide. *J. Phys. Chem. A* 102, 6643–6650.
- Maier, G., Eckwert, J., Bothur, A., Reisenauer, H.P., Schmidt, C., 1996. Photochemical fragmentation of unsubstituted tetrazole, 1,2,3-triazole, and 1,2,4-triazole: first matrix-spectroscopic identification of nitrilimine HCNNH. *Liebig's Ann.* 7, 1041–1053.
- Masterson, C.M., Khanna, R.K., 1990. Absorption intensities and complex refractive indices of crystalline HCN, HC₃N, and C₄N₂ in the infrared region. *Icarus* 83, 83–92.
- Matthews, C.N., 1995. Hydrogen cyanide polymers: from laboratory to space. *Planet. Space Sci.* 43, 10–11, 1365–1370.
- Mielke, A., Andrews, L., 1990. Matrix infrared studies of the HCN + O₃ and HCN + O systems. *J. Phys. Chem.* 94, 3519–3515.
- Milligan, D.E., Jacox, M.E., 1964. Infrared spectrum of HCO. *J. Chem. Phys.* 41, 3032–3036.
- Milligan, D.E., Jacox, M.E., 1967a. Infrared and ultraviolet spectroscopic study of the products of the vacuum-ultraviolet photolysis of methane

- in Ar and N₂ matrices. The infrared spectrum of the free radical CH₃. *J. Chem. Phys.* 47, 5146–5156.
- Milligan, D.E., Jacox, M.E., 1967b. Spectroscopic study of the vacuum-ultraviolet photolysis of matrix-isolated HCN and halogen cyanides. infrared spectra of the species CN and XNC. *J. Chem. Phys.* 47, 278–285.
- Moore, C.B., Pimentel, G.C., 1963. Infrared spectrum and vibrational potential function of ketene and deuterated ketenes. *J. Chem. Phys.* 38, 2816–2829.
- Moore, C.B., Pimentel, G.C., Goldfarb, T.D., 1965. Matrix photolysis products of diazomethane: Methyleneimine and hydrogen cyanide. *J. Chem. Phys.* 43, 63–70.
- Moore, M.H., Donn, B., Khanna, R., A'Hearn, M.F., 1983. Studies of proton-irradiated cometary-type-ice mixtures. *Icarus* 54, 388–405.
- Moore, M.H., Hudson, R.L., 1998. Infrared study of ion-irradiated water ice mixtures with organics relevant to comets. *Icarus* 135, 518–527.
- Moore, M.H., Hudson, R.L., 2000. IR detection of H₂O₂ at 80 K in ion-irradiated laboratory ices relevant to Europa. *Icarus* 145, 282–288.
- Moore, M.H., Hudson, R.L., Gerakines, P.A., 2001. Mid- and far-infrared spectroscopic studies of the influence of temperature, ultraviolet photolysis and irradiation on cosmic-type ices. *Spectrochim. Acta* 57, 843–858.
- Ogilvie, J.F., 1968. Vibrational absorption of the trapped diazomethyl radical. *Can. J. Chem.* 46, 2472–2474.
- Ohishi, M., Kaifu, N., 1998. Chemical and physical evolution of dark clouds. Molecular spectral line survey toward TMC-1. *Faraday Discuss.* 109, 205–216 Cambridge, UK.
- Oro, J., 1960. Synthesis of adenine from ammonium cyanide. *Biophys. Res. Commun.* 2, 407–412.
- Oro, J., Lazcano-Araujo, A., 1981. The role of HCN and its derivatives in prebiotic evolution. Vennesland, B., Conn, E.E., Knowles, E.J., Westley, J., Wissing, F. (Eds.), *Cyanide in Biology*. Academic Press, London.
- Owen, T.C., Roush, T.L., Cruikshank, D.P., Elliot, J.L., Young, L.A., deBergh, C., Schmitt, B., Geballe, T.R., Brown, R.H., Bartholomew, M.J., 1993. Surface ices and the atmospheric composition of Pluto. *Science* 261, 745–748.
- Pacansky, J., Horne, D.E., Gardini, G.P., Bargon, J., 1977. Matrix-isolation studies of primary alkyl radicals. *J. Phys. Chem.* 81, 2149–2154.
- Peyron, M., Broida, H.P., 1959. Spectra emitted from solid nitrogen condensed at very low temperatures from a gas discharge. *J. Chem. Phys.* 30, 139–150.
- Quirico, E., Doute, S., Schmitt, B., de Bergh, C., Cruikshank, D.P., Owen, T.C., Geballe, T.R., Roush, T.L., 1999. Composition, physical state, and distribution of ices at the surface of Triton. *Icarus* 139, 159–178.
- Rodgers, S.D., Charnley, S.B., 1998. HNC and HCN in comets. *Astrophys. J. Lett.* 501, 227–230.
- Satorre, M.A., Palumbo, M.E., Strazzulla, G., 2001. Infrared spectra of N₂-rich ice mixtures. *J. Geophys. Res.* 106, 33363–33370.
- Sandford, S.A., Bernstein, M.P., Allamandola, L.J., Goorvitch, D., Teixeira, T.C.V.S., 2001. The abundances of solid N₂ and gaseous CO₂ in interstellar dense molecular clouds. *Astrophys. J.* 548, 836–851.
- Scott, T.A., 1976. Solid and liquid nitrogen. *Phys. Rep.* 27, 87–157.
- Seburg, R.A., McMahon, R.J., 1992. Photochemistry of matrix-isolated diazoethane and methyldiazirine: ethylidene trapping. *J. Am. Chem. Soc.* 114, 7183–7189.
- Strazzulla, G., Calcagno, L., Foti, G., 1984. Build up of carbonaceous material by fast protons on Pluto and Triton. *Astron. Astrophys.* 140, 441–444.
- Strazzulla, G., Baratta, G.A., Palumbo, M.E., 2001. Vibrational spectroscopy of ion-irradiated ices. *Spectrochim. Acta* 57, 825–842.
- Strazzulla, G., Palumbo, M.E., 2001. Organics produced by ion irradiation of ices: some recent results. *Adv. Space Res.* 27, 237–243.
- Theophanides, T., Turrell, G.C., 1967. Infrared study of thermal decomposition of the azide ion. *Spectrochim. Acta* 23, 1927–1935.
- Thompson, W.R., Murray, B.G.J.P.T., Khare, B.N., Sagan, C., 1987. Coloration and darkening of methane clathrate and other ices by charged particle irradiation: applications to the outer Solar System. *J. Geophys. Res.* 92, 14933–14947.
- Tian, R., Facelli, J.C., Michl, J., 1988. Vibrational and electronic spectra of matrix-isolated N₃⁺ and N₃⁻. *J. Phys. Chem.* 92, 4073–4079.
- Tielens, A.G.G.M., Hagen, W., 1982. Model calculations of the molecular composition of interstellar grain mantles. *Astron. Astrophys.* 114, 245–260.
- Wöhler, F., 1828. On the artificial production of urea. *Ann. Phys. Chem.* 12, 253–256.